Medicine in Novel Technology and Devices 16 (2022) 100174

Contents lists available at ScienceDirect

Medicine in Novel Technology and Devices

journal homepage: www.journals.elsevier.com/medicine-in-novel-technology-and-devices/

Full Length Article

Evaluation of temperature distribution for bone drilling considering aging factor

Huanxin Wang [a], Xiangsheng Gao [a,*], Boxu Wang [a], Min Wang [a,b], Yunan Liu [c,**], Tao Zan [a], Peng Gao [a], Chaozong Liu [d]

[a] Beijing Key Laboratory of Advanced Manufacturing Technology, Faculty of Materials and Manufacturing, Beijing University of Technology, Beijing, 100124, China
[b] Beijing Key Laboratory of Electrical Discharge Machining Technology, Beijing, 100191, China
[c] Beijing Key Lab of Environmental Noise and Vibration, Institute of Urban Safety and Environmental Science, Beijing Academy of Science and Technology, Beijing, 100054, China
[d] Division of Surgery & Interventional Science, University College London, Royal National Orthopaedic Hospital, London, HA74LP, United Kingdom

A R T I C L E I N F O

Keywords:
Cortical bone
Bone drilling
Temperature field
FEM
Aging factor

A B S T R A C T

Bone drilling is a routine operation in surgeries, such as neurosurgery and orthopedics. However, the excessive drilling temperature may cause severe thermal damage to the bone tissue. Therefore, the drilling temperature determination of bone tissue can reduce the harm caused by thermal damage. A time-varying temperature field simulation model of bone drilling was set up by ABAQUS software in this paper, based on the Johnson-Cook model. Then it was validated with experiments by drilling cortical bone of fresh bovine shaft of the femur. The relative error between the experimental values and the theoretical values within 7.67% showed a good consistency. Furthermore, the aging factor is also considered to evaluate the temperature field of bone drilling. The results showed that the drilling temperature near the bone-drill area increased significantly. The drilling temperature of cortical bone decreases sharply with the radial distance and exhibits a hysteresis lag in the axial distribution. The aging factor mainly affects the peak of drilling temperature. The peak of drilling temperature tends to increase with age. The peak drilling temperature in the elderly (70y) was up to 6.8% higher than that in the young (20y), indicating that the elderly is more prone to excessive drilling temperature. Therefore, special attention should be paid to the temperature control of elderly bone tissue.

1. Introduction

Bone drilling is a routine operation in surgeries, such as neurosurgery and orthopedics. The drilling temperature of bone tissue increases sharply because of the strain and friction between twist drill and bone tissue. Bone is a special connective tissue, which exposure to more than 47 °C for 1 min will cause irreversible thermal damage [1–3], thus affecting the success rate of surgery and recovery period. Therefore, study on the temperature of bone drilling is necessary. The physical and geometrical characteristics of the human bone tissue change with aging. The aging process of human is usually accompanied by impaired bone tissue function. Bone tissue damage and aging are also correlated to increased incidence of osteoporosis and fracture in the elderly [4]. The mechanical and thermal properties of bone tissue at different ages are different, and the temperature distribution during bone drilling is also different. Therefore, the aging factor should also be considered in the evaluation of the temperature field of bone drilling.

In recent years, researches on bone drilling temperature have been carried out, including research on thermal damage on bone tissue, comparison of bone drilling technology, and prediction of tissue drilling temperature, etc., which can be divided into experimental method, finite element method and analytical method.

There are two common methods to measure the drilling temperature of bone tissue: infrared thermography and thermocouple. The highest temperature often occurs in the part where the drill is in contact with the drilled material. Infrared thermography is a noninvasive temperature measurement technique for measuring the surface temperature of an object according to the thermal energy [5], so it is used to measure the temperature directly at the bone-drill area [6]. A. Robles et al. [7] found that when bone tissue is drilled at high temperature, the necrotic depth is

* Corresponding author.
** Corresponding author.
E-mail addresses: gaoxsh@bjut.edu.cn (X. Gao), longtang2046@bmilp.com (Y. Liu).

https://doi.org/10.1016/j.medntd.2022.100174
Received 22 July 2022; Received in revised form 30 August 2022; Accepted 6 September 2022

8 times larger than that of conventional drilling, and the brittleness of bone tissue increases while the stiffness and strength decrease. Khurshid Alam et al. [8] found that the abrasion of the drill has a strong correlation between the temperature, torque, drilling force, and surface roughness of the borehole, and the feed rate is the principal factor, and then the roughness of the drill. The drill with certain rotational speed and feed rate is effective for safe bone drilling. Hihao Li et al. [9] found that the cutting lip, and the drilling time may mainly affect the peak temperature. Besides, there is no phenomenon of anisotropy on the temperature distribution was discovered. Thermocouples is an invasive temperature measurement technique which bases on the Seebeck effect to measure the internal temperature of objects [10], so it is used to measure the temperature inside of the objects. Andrew C. Palmisano et al. [11] found that cannulated drill generated the highest temperature and twist drills generated the smallest temperature. Twist drills have a growing tendency with size and thermogenesis. However, the size of K wires was not significant. Goran Augustin et al. [12] found that drilling temperature was below the critical 47 °C with internal cooling. Even using the 4.5 mm drill without cooling with water and with low feed rates, the temperature was below critical. However, due to physical limitations, the thermocouples can only be placed in a fixed position near the hole, and information cannot be collected adequately by experiments of bone drilling.

Nowadays, analytical method and FEM are mainly used to predict temperature distribution during bone drilling, and the results are verified by experiments. However, the analytical method depends on the model, and different models may lead to different results, so it is necessary to verify the correctness of the model through experiments. Hossein H. Hassanalideh et al. [13] found that coolants and drilling angles are mainly factors with HSS drill and stainless steel drill during bone drilling. Ali Akhbar et al. [14] found that the maximum temperature increased with rotational speed, drilling hole depth and drill diameter. But thermal damage can be reduced by increasing the feed rate. Sinan Liu et al. [15] found that the thrust force and temperature can be efficiently reduced by using crescent drill even without coolant. Hamed Heydari et al. [16] presented an analytical model based on Sui and Sugita model and found that drilling force mainly affects drilling temperature. The maximum drilling temperature decreases with drilling force and then increases. Yahui Hu et al. [6] employed the moving heat source method and found that due to the low thermal conductivity of the cortical bone, the temperature of the cortical bone decreased with the radial distance. The FEM is also model-dependent, but can be used to simulate more complex situations. Maziar Aghvami et al. [17] established a mathematical model of heat transfer of different densities and found that the theoretical critical temperature of thermal damage was 47 °C. The thermal damage is mainly determined by the drill diameter and drilling speed.

At present, cells from the bone tissue, structure, and micro-level, etc., are mainly used to explain the variation of temperature change. Although there are some experimental samples including bone tissue of different ages, the difference in drilling temperature caused by the microstructure change of bone tissue with aging was not considered. Addolorata Corrado et al. [4] studied the pathogenesis of aging bones at a molecular level, and investigated the theories of bone aging including systemic and local factors. The incidence of fracture of bone aging increases with the variations at cellular, tissue and structural levels. Cheng Duan [18] considered the effects of the aging factor on femoral geometric parameters and material parameters to establish a multi-age finite element model, and showed that the elastic modulus, ultimate stress and ultimate strain of cortical bone of the femur decreased gradually with aging. And the aging factor also influenced the size and shape of the femur. Aleksa Marković [19] studied the changes in temperature of the adjacent low-density bone during implant placement and found that age, gender, bone density nor cortical bone thickness had no statistically significant effect on bone thermal changes during the implantation procedure compared with different surgical method.

The previously relevant studies of bone drilling temperature focused on the maximum drilling temperature, the effects from bone drilling technology, however, these cursory studies do not reflect the distribution and changes of drilling temperature considering the aging factor. The thermal damage of bone tissue is a time-dependent phenomenon, so in this paper, a time-varying temperature field simulation model during bone drilling was established by ABAQUS software, considering a single-factor node solution to analyze the temperature distribution. Then it was validated with experiments by drilling cortical bone of fresh bovine shaft of the femur. Due to the great difference of bone tissue in different age stages, the aging factor is also considered to evaluate the temperature field of bone drilling, which then can control better temperature during bone drilling.

2. Bone drilling simulation model

2.1. Model setup

2.1.1. Model design

A twist drill model with a diameter of 3 mm was established using SOLIDWORKS software, and then imported into ABAQUS software. A bone model with a square of 16 mm and a thickness of 6 mm was also built. 9 concentric circles with a radius from 2 mm to 6 mm were drawn at the center of the surface of the bone model and stretched along the z-axes. The assembly drawing of the drilling model is shown in Fig. 1a.

2.1.2. Model material

The drill material was stainless steel 4Cr13, and the drilled material is cortical bone of the femur. Cortical bone is an anisotropic material. However, there is no phenomenon of anisotropy on the temperature distribution was discovered [9,20]. Therefore, cortical bone was considered as isotropic material in this paper. Table 1 presents the material parameters of twist drill and cortical bone [21].

Johnson-Cook model is one of the models to predict the mechanical behavior of cortical bone material with high temperature and strain rate [6]. In this paper, Johnson-Cook model is used as constitutive model. The flow stress equation [21] can be expressed as follows:

$$\sigma = (A + B\cdot\varepsilon^n)\left[1 + C\cdot\ln\left(\frac{\overline{\varepsilon}}{\overline{\varepsilon}_0}\right)\right]\left[1 - \left(\frac{T - T_r}{T_m - T_r}\right)^m\right] \tag{1}$$

where σ is the flow stress, A, B, C are the material constants, n, m are the strain hardening exponent, ε is the effective plastic strain,ε is the effective plastic strain rate, ε_0 is the static plastic strain rate, T_m is the melting temperature, T_r is the room temperature. Table 2 presents the detail model parameters [21].

2.1.3. Mesh grid of model

The mesh grid of the drilling model is shown in Fig. 1a. The drill model was meshed into the tetrahedral element, and the total number of elements is 11,568. The bone model was meshed into hexahedral element, 50 nodes were set on each drawn concentric circle and the total number of elements is 13,643.50 nodes on each concentric circle (same radial distance and axial depth) were set as a node-set, and the total number of node sets was 108 groups. The node-set of the drilling model is shown in Fig. 1b.

2.1.4. Boundary condition setup and solving process

The boundary condition setup of the bone drilling model is shown in Fig. 1c. Fixed boundary of the bone model on the X and Y direction to simulate the state of the bone tissue being fixed on the workbench. The drill was rotated on the Z-axes and the feed direction was set to the Z direction. The spindle speed of the drill was 1000 r/min and the feed rate was 80 mm/min. The initial temperature of bone tissue and twist drill was 25 °C to simulate the ambient temperature (Beijing, China).

The drill was set to rigid model [13]. The interaction between the

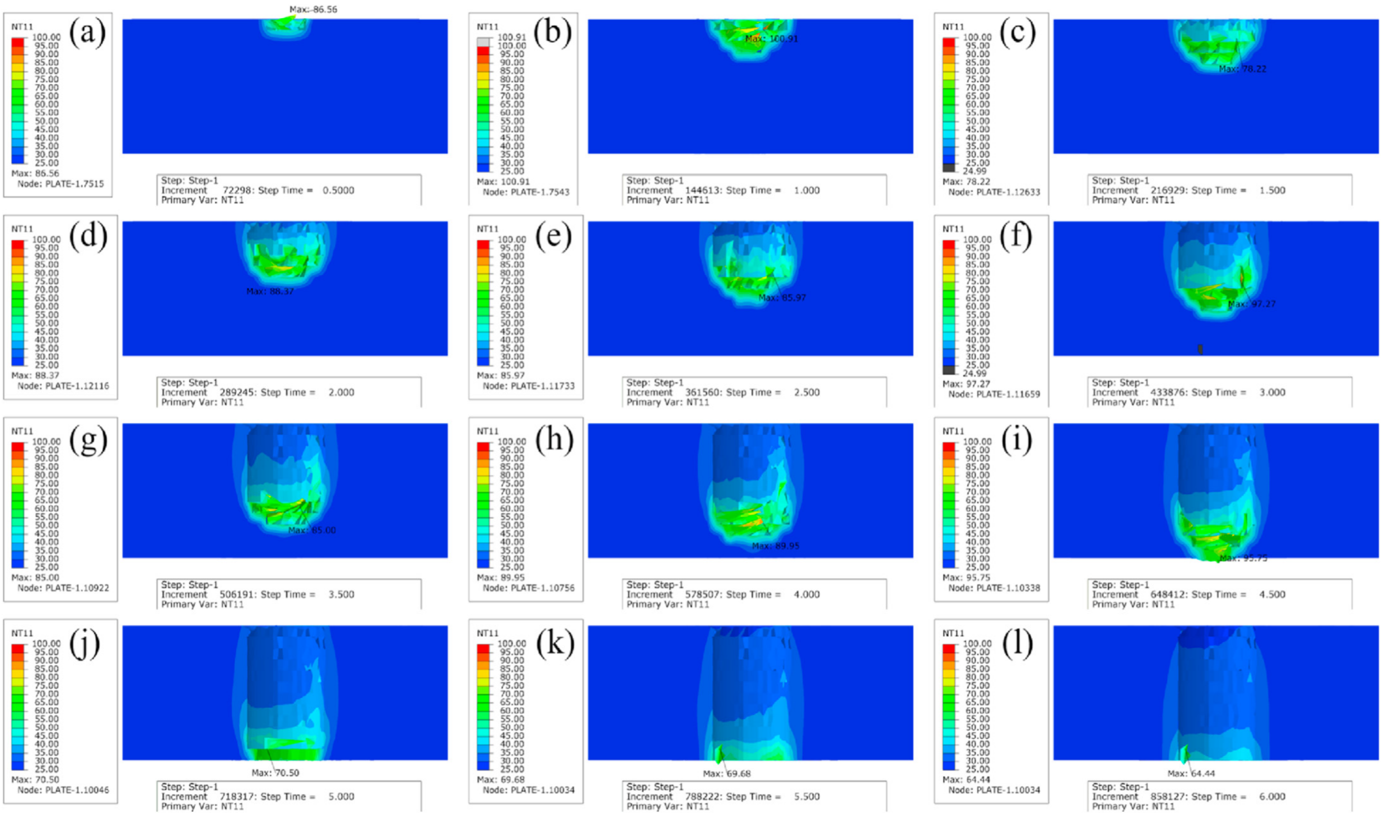

Fig. 1. (a) Assemble and mesh grid. (b) Node-set. (c) Boundary condition setup.

Table 1
Material parameters of twist drill and cortical bone [21].

Parameters	Twist Drill	Cortical Bone
Density (kg/m^3)	7840	2000
Young's Modulus (GPa)	21.0	20.0
Poisson's Ratio	0.3	0.36
Yielding Strength (MPa)	585	106
Specific Heat (J/kg·K)	460	1640
Thermal Conductivity (W/m·k)	29.0	0.56

Table 2
Johnson-Cook material of cortical bone [21].

A (MPa)	B (MPa)	C	n	M	T_m (°C)
50	101	0.03	0.08	1.03	1300

twist drill and bone tissue was assigned with surface-to-surface contact (Explicit) option, and the solution was obtained by the dynamic temperature-displacement step.

2.1.5. *Model results and discussion*

The average temperature variation in each node-set was taken as the result of this position to obtain the variation of the drilling temperature field, as shown in Fig. 2. During bone drilling, the temperature near the bone-drill area increased significantly. The high temperature mainly appeared near the cutting edge. According to Fig. 2b, the maximum temperature could reach 100.9 °C. During bone drilling, the bone tissue in the drilling area was damaged by drill, which generated aplenty drilling heat and moved with the drill feed movement.

During bone drilling, the distribution of drilling temperature was mainly related to the radial distance and axial depth between the node and the drilling center. At the same radial distance and axial depth, the drilling temperature difference between nodes was not obvious.

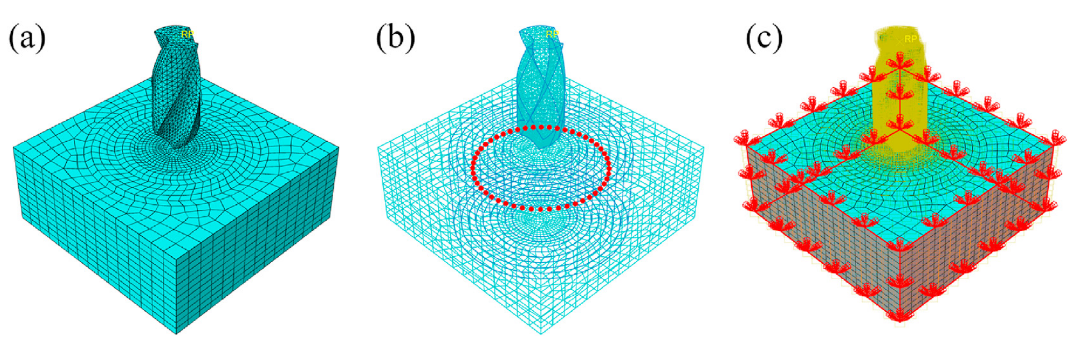

Fig. 2. Drilling temperature.

Table 3
Single factor solution of drilling temperature.

Parameters	Numerical Value
Radial Distance r (mm)	2.0, 2.5, 3.0, 3.5, 4.0, 4.5, 5.0, 5.5, 6.0
Axial Depth d (mm)	0.5, 1.0, 1.5, 2.0, 2.5, 3.0, 3.5, 4.0, 4.5, 5.0, 5.5, 6.0

Therefore, a single-factor node solution scheme was designed in this paper, as shown in Table 3.

To observe the drilling temperature distribution, the variation of drilling temperatures over time at different radial distances and axial depths were compared, as shown in Fig. 3. The drilling temperature increased sharply and then decreased slowly, and the maximum temperature was 40.1 °C, which occurred at 5.72 s, as shown in Fig. 3l. The temperature with a radial distance of 2.0 mm changed dramatically. In terms of radial distance, the temperature peak showed a non-linear sharp decline trend with non-uniformity. In terms of axial depth, the peak time had a hysteresis effect, and the temperature peak tended to increase slightly with uniformity. Due to the low conductivity of the bone tissue, drilling heat was easy to accumulate in the drilling area, which could not be diffused effectively. So, the temperature in drilling area changed obviously, and the distant area changed barely. The greater the distance from the drilling center, the higher the maximum drilling temperature that can be achieved. At the same time, the heat source is in a constant motion, the distance between each node and the heat source increases firstly and then decreases, so the drilling temperature also shows a trend of increasing firstly and then decreasing. The excessive drilling temperature occurred at the drilling area should be considered in the design of cooling methods.

2.2. Experimental test

2.2.1. Experimental material

Because of the limitations of experimental conditions and ethics, the human bone could not be used as experimental material in this paper. The bovine bone resembles in terms of material properties and mechanical properties [7,9,20], so using fresh bovine femurs in this experiment. The bones were purchased from a local slaughterhouse and had been cut into segments. To ensure the accuracy of the experiment, the selected cortical bone thickness of bovine bone samples was about 6 mm. The surface soft tissue of the bovine bone sample was disposed and only the middle part of bone was reserved as experimental material, to be fixed and installed. A twist drill of 4Cr13 stainless steel was used to conduct the drilling.

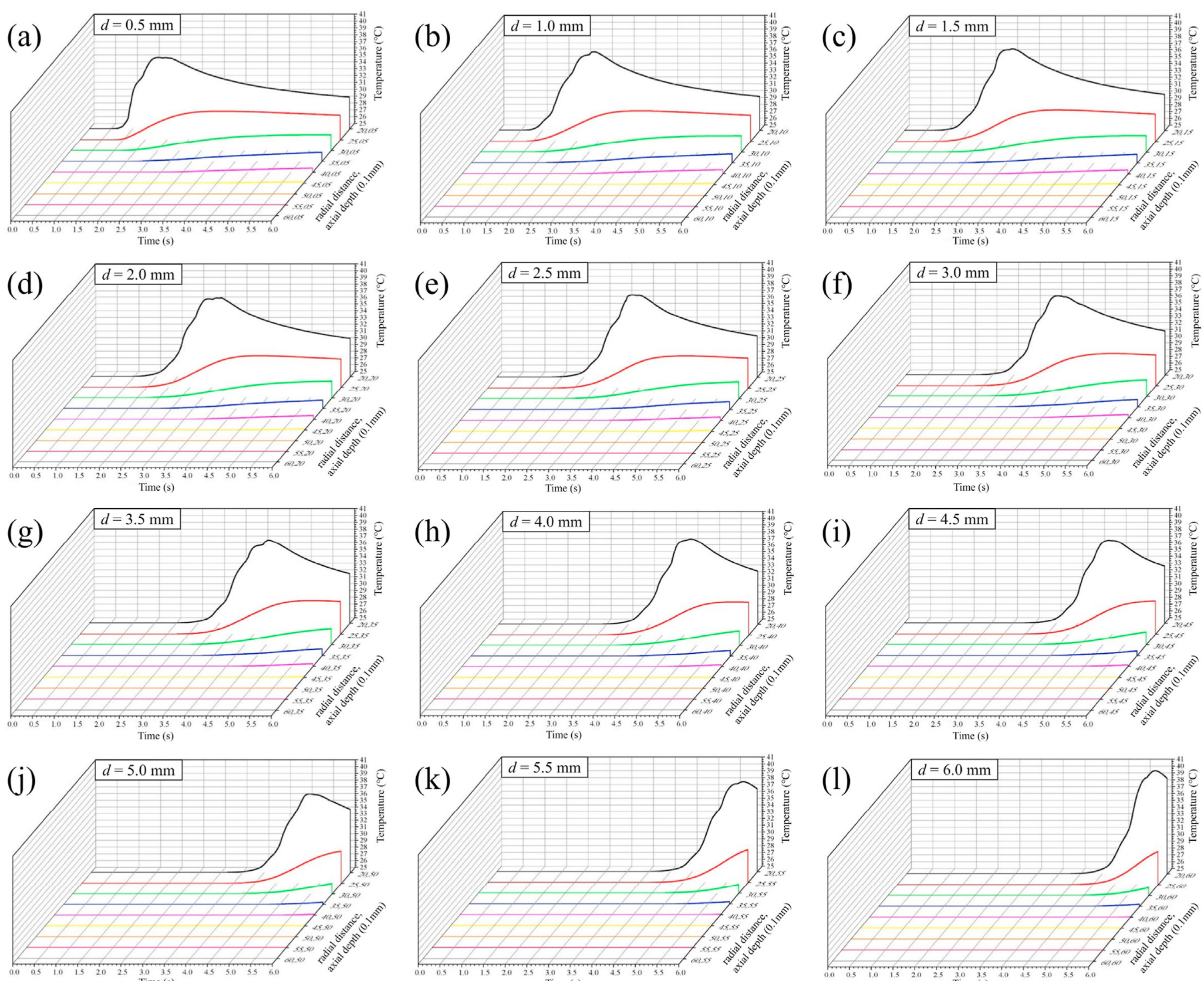

Fig. 3. Drilling temperatures at different radial distances and axial depths.

2.2.2. Experimental system

The drilling experiments were conducted on a V5 Numerical Control Machines (Siemens system). K-type thermocouple is used to measure the temperature inside the cortical bone. An ADAM-17 acquisition card and LABVIEW software were used to collect the temperature during bone drilling, with a sampling frequency of 50Hz.

2.2.3. Experimental design

The temperature distribution with different radial distances inside of the cortical bone was investigated in the same conditions (drill diameter, spindle speed, feed rate, and room temperature are 3 mm, 1000 r/min, 80 mm/min, 25 °C, respectively). The experimental design is shown in Table 4. A schematic diagram of bone drilling experiment system is shown in Fig. 4a, *D* is the twist drill diameter, *h* is the axial depth of the twist drill, and *r* is the radial distance between the temperature measured point (TMP) and the axis of the drill. And cortical bone drilling experiment system is shown in Fig. 4b.

Table 4
Experimental design at different temperature measured point.

Number	Drill Diameter *D* (mm)	Spindle Speed *n* (r/min)	Feed Rate *v* (mm/min)	Radial Distance *r* (mm)	Axial Depth *d* (mm)
1	3	1000	80	2.0	6
2				2.5	

2.2.4. Experimental results and discussion

The cortical bone drilling experiments were conducted according to the experimental design. The temperature was recorded by ADAM-17 acquisition card and LABVIEW software. The experimental results under the same drilling conditions were compared with the theoretical results to verify the accuracy of the drilling simulation model. The experimental and simulated results of drilling temperature under different measuring positions are shown in Fig. 5. The experimental results were in good agreement with the simulated results.

The experimental and simulated values of cortical bone temperature at different temperature measured point are shown in Table 5. When the drill diameter was 3 mm, spindle speed was 1000 r/min, the feed rate was 80 mm/min, the radial distance was 2.0 mm, and the peak temperature was up to 36.47 °C. Furthermore, the maximum relative error between the experimental values and the simulated values was 6.74%. When the radial distance was 2.5 mm, the peak temperature was up to 29.69 °C, and the maximum relative error between the experimental values and the simulated values was 7.67%, the results obtained in the experiments were larger than the simulated values. This error is likely because the actual radial distance of the thermocouples was slightly less than the experimental design value. The peak temperature decreased

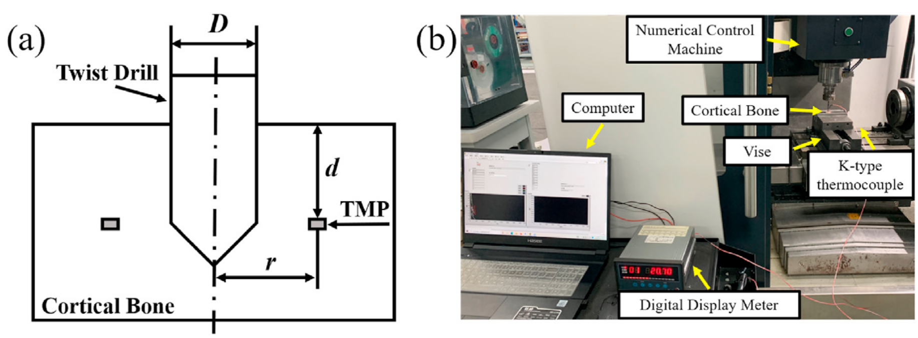

Fig. 4. (a) Schematic diagram. (b) Cortical bone drilling test system.

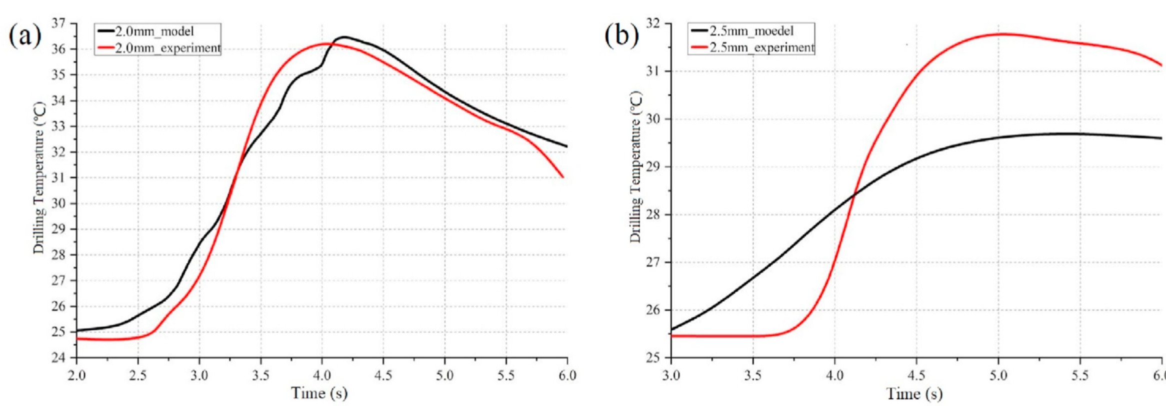

Fig. 5. Experimental and simulated results of drilling temperature.

Table 5
Experimental and simulated values of drilling temperature.

Number	Radial Distance *r* (mm)	Peak	Model Values	Experimental Values	Relative Error	Maximum Relative Error
1	2.0	Temperature	36.47 °C	36.22 °C	0.67%	6.74%
		Time	4.18s	3.96s	5.26%	–
2	2.5	Temperature	29.69 °C	31.79 °C	7.08%	7.67%
		Time	5.42s	5.04s	7.01%	–

Table 6
Material parameters of cortical bone at different age stages.

Age (year)	Density (kg/m^3)	Young's Modulus (GPa)	Ultimate Stress (%)	Ultimate Strain (MPa)
20	1883	16.83	120.4	3.57
30	1856	16.24	115.2	3.24
40	1830	15.65	110.0	2.91
50	1803	15.06	104.8	2.58
60	1777	14.47	99.6	2.25
70	1750	13.88	94.4	1.92

sharply with the radial distance. In this paper, because the size of the thermocouples was slightly smaller than the pre-bored hole, there were errors at the actual temperature measured point, and the thermocouple holes created unnecessary interferences for the heat dissipation in bone tissue, then influencing the temperature distribution near the borehole. Moreover, as the material parameters of the model are theoretical data obtained from the literature rather than actual tests, which may be different from the actual experimental materials, also may lead to errors between the experimental and theoretical values.

With the radial distance of 2.0 mm, the drilling temperature increased rapidly at about 2.5 s, reached the peak at about 4.0 s and then decreased. With the radial distance of 2.5 mm, the drilling temperature increased at about 3.5 s, reached the peak at about 5.0 s and then decreased slowly. The results showed that the closer the radial distance was, the more drastic change of drilling temperature was.

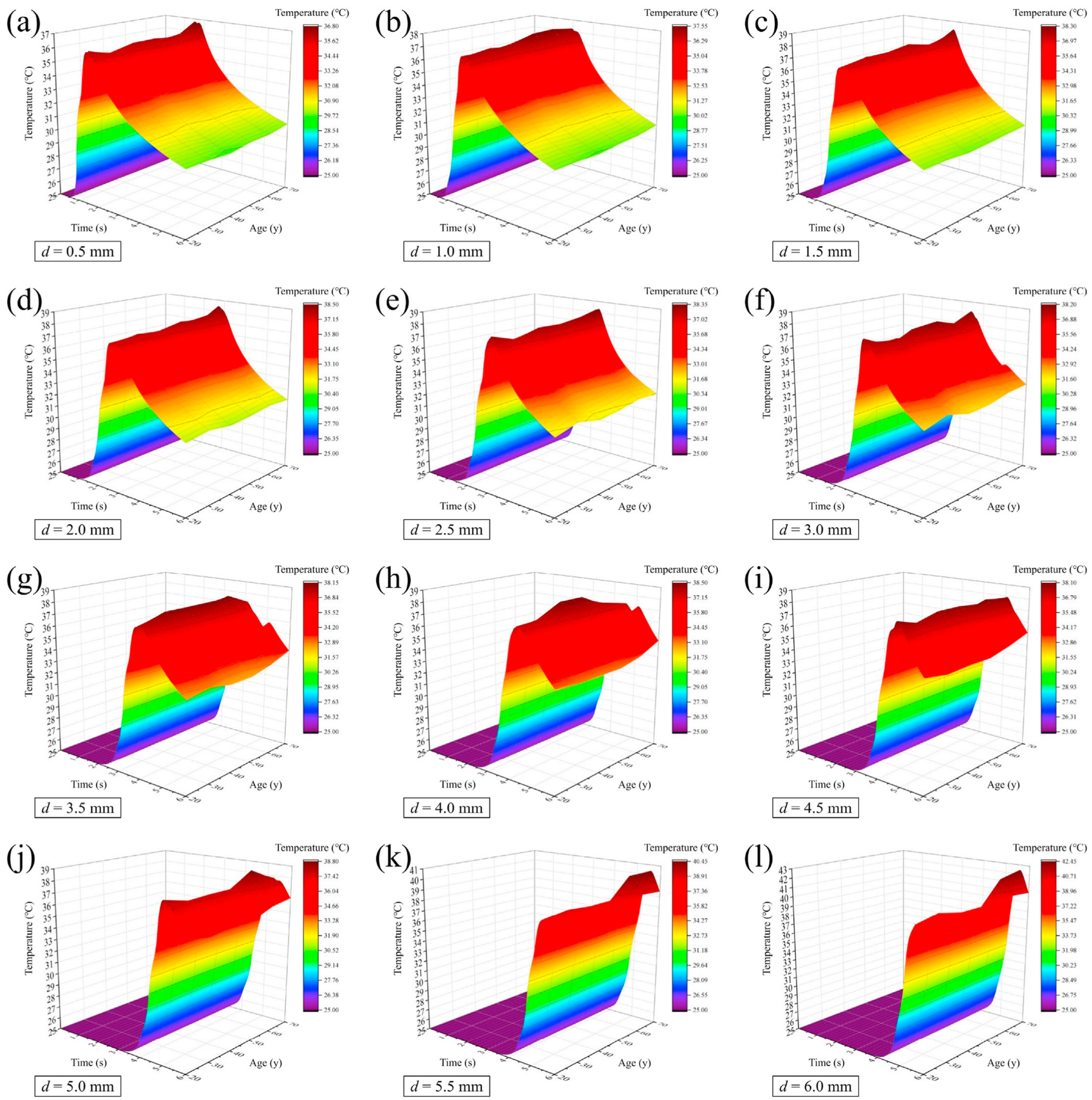

Fig. 6. Drilling temperatures at different age stages and axial depth.

3. Bone drilling model considering the aging factor

3.1. Aging factor

Bone tissue varies with aging at the cellular, tissue and structural levels [7,18,22]. The material parameters of cortical bone such as density and elastic modulus decreased linearly with aging [18,22]. After simple linear regression analysis of cortical bone material parameters, a linear equation of density, elastic modulus, ultimate stress and ultimate strain with aging can be calculated as follows:

$$\begin{cases} \rho = 1935.6 - 2.65x \\ E = 18.01 - 0.059x \\ \sigma_u = 130.8 - 0.52x \\ \varepsilon_u = 4.23 - 0.033x \end{cases} \quad (2)$$

where x is the age, ρ is the density, E is the Young's modulus, σ_u is the ultimate stress, ε_u is the ultimate strain.

Material parameters of cortical bone of 6 groups at different age stages with intervals of 10 years were obtained by Eq. (2), as shown in Table 6. The material parameters of the bone model in the 6 groups are introduced into the bone drilling model respectively.

3.2. Simulated results and discussion

The variation of drilling temperatures over time at different age stages and axial depths were obtained by ABAQUS software. With the radial distance of 2.0 mm, the temperature changed obviously, so the variation of drilling temperature with the radial distance of 2.0 mm at different age stages was compared, and the trend of peak temperature and peak time with aging was also analyzed. The results showed that the temperature peak at different axial depths increases with aging.

As shown in Fig. 6, the temperature peak almost appeared at the age of 70, and the maximum peak temperature was up to 42.4 °C. As shown in Fig. 6l, the peak temperature increased by 6.8% compared with 39.7 °C at the age of 20, but was lower than the critical temperature of thermal damage. Moreover, the peak time at different radial depths was almost unchanged. The results showed that aging factor mainly affect the value of drilling temperature. From the point of view of parameter variation, the change of material parameters of bone tissue led to the concentration of energy at drilling area, which could not be diffused easily, so the temperature increased slowly. The elderly is prone to excessive temperature during bone drilling and are more likely to reach the critical temperature with thermal damage. Therefore, special attention of temperature controlling should be paid to the elderly during bone drilling.

4. Conclusion

In this paper, a time-varying temperature field simulation model of bone drilling was established by finite element method, the distribution of drilling temperature was studied, and the main factors affecting the distribution of drilling temperature were analyzed according to the results. The drilling model was verified by drilling experiment of bovine femur. The influence of aging factor on the peak temperature and peak time was mainly considered and discussed. The following conclusions from the present work are listed.

(1) The drilling temperature firstly increases sharply and then decreases slowly with time. The peak temperature shows a non-linear sharp decline trend with non-uniformity varied with radial distance. The peak time has a hysteresis effect, and the peak temperature tends to increase slightly with uniformity varied with axial depth,.
(2) The relative error between the experimental values and the simulated values is within 7.67%. The temperature distribution during bone drilling could be predicted accurately by this drilling model.
(3) The aging factor mainly affects the value of drilling temperature, and the elderly are prone to excessive temperature during bone drilling and are more likely to reach the critical temperature with thermal damage.

Since this model analyzes the influence of aging factors on bone tissue drilling from the perspective of mechanical engineering, however, bone tissue is an active and composite material, it may be necessary to combine biology and material science to further analyze the cause and mechanism of temperature change. In addition, in-vivo study on bone drilling may be the future study in this research direction.

Funding

This study was supported by the National Natural Science Foundation of China (grant numbers: 51,875,008 and 52,105,424), R&D Program of Beijing Municipal Education Commission (KM202210005033), Royal Society via an International Exchange programme (Grant No: IEC\NSFC\191,253), International Research Cooperation Seed Fund of Beijing University of Technology (grant number: 2021A10), BJAST Innovation Cultivation Programes (No. 11000022T000000446498), and BJAST Budding Talent Program (BGS202210).

Funding source

All sources of funding should also be acknowledged and you should declare any involvement of study sponsors in the study design; collection, analysis and interpretation of data; the writing of the manuscript; the decision to submit the manuscript for publication. If the study sponsors had no such involvement, this should be stated.

Please state any sources of funding for your research:

National Natural Science Foundation of China (grant numbers: 51875008 and 52105424), R&D Program of Beijing Municipal Education Commission (KM202210005033), Royal Society via an International Exchange programme (Grant No: IEC\NSFC\191,253), International Research Cooperation Seed Fund of Beijing University of Technology (grant number: 2021A10), BJAST Innovation Cultivation Programes (No. 11000022T000000446498), and BJAST Budding Talent Program (BGS202210).

References

[1] Eriksson AR, Albrektsson T, Grane B, McQueen D. Thermal injury to bone: a vital-microscopic description of heat effects. Int J Surg 1982;11(2):115–21. https://doi.org/10.1016/S0300-9785(82)80020-3.
[2] Eriksson AR, Albrektsson T. Temperature threshold levels for heat-induced bone tissue injury: a vital-microscopic study in the rabbit. J Prosthet Dent 1983;50(1): 101–7. https://doi.org/10.1016/0022-3913(83)90174-9.
[3] Eriksson RA, Albrektsson T. The effect of heat on bone regeneration: an experimental study in the rabbit using the bone growth chamber. J Oral Maxillofac Surg 1984;42(11):705–11. https://doi.org/10.1016/0278-2391(84)90417-8.
[4] Corrado A, Cici D, Rotondo C, Maruotti N, Cantatore FP. Molecular basis of bone aging. Int J Mol Sci 2020;21(10):3679. https://doi.org/10.3390/ijms21103679.
[5] Kus A, Isik Y, Cakir MC, Coşkun S, Özdemir K. Thermocouple and infrared sensor-based measurement of temperature distribution in metal cutting. Sensors 2015; 15(1):1274–91. https://doi.org/10.3390/s150101274.
[6] Hu Y, Ding H, Shi Y, Zhang H, Zheng Q. A predictive model for cortical bone temperature distribution during drilling. Phys Eng Sci Med 2012;44(1):147–56. https://doi.org/10.1007/s13246-020-00962-4.
[7] Robles-Linares JA, Axinte D, Liao Z, Gameros A. Machining-induced thermal damage in cortical bone: necrosis and micro-mechanical integrity. Mater Des 2021; 197:109215. https://doi.org/10.1016/j.matdes.2020.109215.
[8] Alam K, Piya S, Al-Ghaithi A, Silberschmidth V. Experimental investigation on the effect of drill quality on the performance of bone drilling. Biomed Tech 2020;65(1): 113–20. https://doi.org/10.1515/bmt-2018-0184.
[9] Li S, Shu L, Kizaki T, Bai W, Terashima M, Sugita N. Cortical bone drilling: a time series experimental analysis of thermal characteristics. J Manuf Process 2021;64: 606–19. https://doi.org/10.1016/j.jmapro.2021.01.046.
[10] Childs PR, Greenwood JR, Long CA. Review of temperature measurement. Rev Sci Instrum 2000;71(8):2959–78. https://doi.org/10.1063/1.1305516.

[11] Palmisano AC, Tai BL, Belmont B, Irwin TA, Shih A, Holmes JR. Comparison of cortical bone drilling induced heat production among common drilling tools. J Orthop Trauma 2015;29(5):e188–93. https://doi.org/10.1097/BOT.0000000000000240.

[12] Augustin G, Davila S, Udilljak T, Staroveski T, Brezak D, Babic S. Temperature changes during cortical bone drilling with a newly designed step drill and an internally cooled drill. Int Orthop 2012;36(7):1449–56. https://doi.org/10.1007/s00264-012-1491-z.

[13] Hassanalideh HH, Gholampour S. Finding the optimal drill bit material and proper drilling condition for utilization in the programming of robot-assisted drilling of bone. CIRP J Manuf Sci Tec 2020;31:34–47. https://doi.org/10.1016/j.cirpj.2020.09.011.

[14] Akhbar MFA, Yusoff AR. Drilling of bone: thermal osteonecrosis regions induced by drilling parameters. Biomed Phys Eng Expr 2019;5(6):065003. https://doi.org/10.1088/2057-1976/ab42f2.

[15] Liu S, Wu D, Zhao J, Yang T, Sun J, Gong K. Novel crescent drill design and mechanistic force modeling for thrust force reduction in bone drilling. Med Eng Phys 2022;103:103795. https://doi.org/10.1016/j.medengphy.2022.103795.

[16] Heydari H, Cheraghi Kazerooni N, Zolfaghari M, Ghoreishi M, Tahmasbi V. Analytical and experimental study of effective parameters on process temperature during cortical bone drilling. Proc Inst Mech Eng H 2018;232(9):871–83. https://doi.org/10.1177/0954411918796534.

[17] Aghvami M, Brunski JB, Serdar Tulu U, Chen CH, Helms JA. A thermal and biological analysis of bone drilling. J Biomech Eng-T ASME 2018;140(10):101010. https://doi.org/10.1115/1.4040312.

[18] Duan Cheng. Structural optimization of implants based on aging factors. Master thesis. Tianjin University of Technology; 2020. https://kns.cnki.net/KCMS/detail/detail.aspx?dbname=CMFD202101&filename=1020137125.nh.

[19] Marković A, Mišić T, Mančić D, Jovanović I, Šćepanović M, Jezdić Z. Real-time thermographic analysis of low-density bone during implant placement: a randomized parallel-group clinical study comparing lateral condensation with bone drilling surgical technique. Clin Oral Implants Res 2014;25(8):910–8. https://doi.org/10.1111/clr.12191.

[20] Xia Lei. Simulation and experimental study of ultrasonically-assisted drilling of cortical bone. Master thesis. Tianjin University of Technology; 2019. https://kns.cnki.net/KCMS/detail/detail.aspx?dbname=CMFD201902&filename=1019902321.nh.

[21] Xiangjun Li. Prediction model of temperature distribution in cortical bone drilling and study of heat affected zone. Master thesis. Tianjin University of Technology; 2019. https://kns.cnki.net/KCMS/detail/detail.aspx?dbname=CMFD201902&filename=1019902338.nh.

[22] Atkinson PJ, Weatherell JA. Variation in the density of the femoral diaphysis with age. J Bone Joint Surg 1967;49(4):781–8 (PMID: 6073195).